J. Phys. B: Atom. Molec. Phys. **13** (1980) 4353–4366. Printed in Great Britain

Experimental determination of the phase differences of continuum wavefunctions describing the photoionisation process of xenon atoms† I. Measurements of the spin polarisations of photoelectrons and their comparison with theoretical results

U Heinzmann

Physikalisches Institut der Universität Münster, D4400 Münster, West Germany and Synchrotron des Physikalischen Instituts der Universität Bonn, West Germany

Received 12 May 1980, in final form 7 July 1980

Abstract. The photoionisation of xenon is completely described by the knowledge of either three or five parameters, corresponding respectively to the $^2P_{1/2}$ and $^2P_{3/2}$ states of the ion, and their dependence on photon energy. In the photon energy range from 12 to 41 eV two of these have been experimentally determined from measurements of the spin polarisation of photoelectrons emitted by unpolarised and circularly polarised VUV radiation. After a description of the apparatus used the measured results are presented and compared with different theoretical results.

1. Introduction

For many years photoionisation or photoemission measurements have been very important methods in the study of the electronic structures of matter. The first measurements performed were of photoionisation cross sections and the energy and angular distributions of photoelectrons. In the last ten years experimental evidence for spin polarisation of photoelectrons has also been obtained (for a review see, for example, Kessler 1976). Such studies of spin polarisation, which arises from the influence of the spin–orbit interaction on the ground, ionic or continuum states, give information on details of the photoionisation or photoemission process which cannot be obtained by other experimental methods.

In the field of atomic physics, spin polarisation measurements and studies of the angular distribution and the cross section complement each other to yield information about the photoionisation process that can, in principle, be complete. In 1969 Fano predicted that photoelectrons emitted by alkali atoms which are exposed to circularly polarised radiation should be polarised (Fano 1969a, b). After this it was not surprising that in other theoretical papers (Cherepkov 1974, 1978, 1979, Lee 1974) the question was discussed, and for certain atoms answered, as to which experimentally obtained photoionisation results are needed to determine all phase differences of the continuum

† Main part of the habilitation thesis (in German) accepted by the Physics Department of the University at Münster.

0022-3700/80/224353+14$01.50

wavefunctions of the photoelectrons as well as matrix elements of the dipole operator describing the transitions into the different energy-degenerate continuum states.

It is the purpose of this paper and the following one (Heinzmann 1980, to be referred to as II) to report on such experimentally obtained phase differences of continuum wavefunctions and matrix elements in the case of the photoionisation of xenon atoms. Xenon has been selected because the rare gases have a simple electronic structure in the ground state (filled shells, total angular momentum $J = 0$). Thus, as pointed out by Cherepkov and Lee, the connection between the photoionisation cross section, the angular distribution and the spin polarization of the photoelectrons on the one hand and the phase differences and matrix elements on the other is not too complicated. Moreover, the rare-gas ions have open shells with the consequence that multi-electron correlations have a non-negligible influence on the photoionisation because of the final-state interaction between the photoelectron and the ion. For the study of these many-electron effects (configuration interaction, channel mixing, autoionisation processes, influences of the spin–orbit interaction) xenon is an especially good example because of its high atomic number.

In this paper discussion is given of Cherepkov's and Lee's prediction as to which spin polarisation results are needed to complete the description of the photoionisation process. Sections 3 and 4 describe the two spin polarisation experiments that have been performed: (i) polarisation of photoelectrons ejected by unpolarised radiation, an experiment in which the photoelectrons are resolved as to angle, energy and spin; (ii) polarisation of photoelectrons produced by circularly polarised radiation, an experiment in which the fact that synchrotron radiation emitted into directions above and below the plane of the synchrotron is largely circularly polarised has been used for the first time. The spin polarisation results reported are compared with theoretical predictions.

In paper II the matrix elements and the phase differences of the wavefunctions, obtained using the experimental results reported here, are shown as functions of the photon energy in the range between the photoionisation threshold and 41 eV. These results are explained and compared with the data below the threshold (obtained by other authors) by use of the 'multichannel quantum defect theory'. The main advantage of this method of describing the absorption of photons by atoms is that the photoionisation threshold is then no longer a threshold between different physical processes. Furthermore, some new aspects of many-electron correlations in the region of autoionisation resonances are found experimentally and discussed.

2. The experimental results needed

Cherepkov (1974, 1978, 1979) and Lee (1974) have specified in their theories the data that are needed for a complete description of the photoionisation process in the non-relativistic approximation, which is valid upto 100 eV photon energy. In the particular cases where either the atom or the remaining ion has filled subshells (rare gases and alkali metals, for example) the photoionisation is completely described by five parameters provided each photoionisation involves only one photon and one photoelectron. The simplification to five parameters is possible only because in these cases the change in the total angular momentum J of the atom is determined unambiguously by the change in the angular momentum j of the electron making the bound–free transition: $J = 0$, $\Delta J = 1$ for the rare gases and $J = j$, $\Delta J = \Delta j$ for the alkalis. The

number five arises from the three real matrix elements and two phase differences associated with the three allowed transitions $\Delta j = 0, \pm 1$. These five parameters, which are functions of the photon energy and the kinetic energy of the photoelectrons, can be determined by five types of measurement.

In the first three types of experiment, unpolarised radiation may be used in the photoionisation. These are the measurement of the following.

(i) The total photoionisation cross section Q describing how many photoelectrons are produced. Q itself is the first parameter.

(ii) The angular dependence of the cross section (differential cross section)

$$Q(\theta) = (Q/4\pi)[1 - \tfrac{1}{2}\beta(\tfrac{3}{2}\cos^2\theta - \tfrac{1}{2})] \tag{1}$$

where θ is the angle between the directions of incoming light and outgoing electron as shown in figure 1. The asymmetry parameter β describes the deviation of the differential cross section from an isotropic form.

(iii) The spin polarisation of the photoelectrons, which is also angle dependent†

$$P(\theta) = \frac{2\xi \sin\theta \cos\theta}{4\pi Q(\theta)/Q}. \tag{2}$$

The direction of the polarisation vector is, for reasons of mirror symmetry, perpendicular to the reaction plane as shown in figure 1. This situation is similar to electron scattering, in which electrons scattered through an angle θ become polarised (Kessler 1976). In contrast to electron scattering $Q(\theta)$ and $P(\theta)$ show π periodicity because in the non-relativistic case (photon momentum negligible with respect to electron momentum) the results do not depend on whether the photon comes from the left or from the right in figure 1. The size of $P(\theta)$ is mainly determined by the parameter ξ; the sign of ξ is defined to be positive for the case drawn in figure 1.

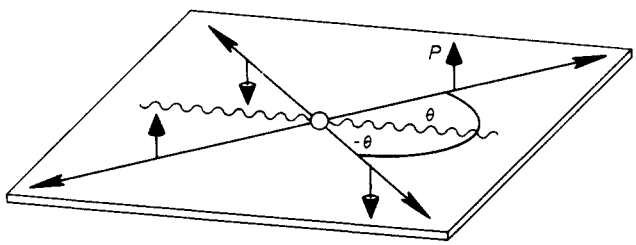

Figure 1. Spin polarisation vector P perpendicular to the reaction plane.

In the fourth and the fifth types of experiment, where circularly polarised radiation has to be used, one observes the spin transfer from the photon to the photoelectron analogous either to the total cross section or the differential cross section.

(iv) Analogous to the total cross section Q there is a total spin polarisation of the photoelectrons A. It is an average value if all the photoelectrons produced are extracted by an electric field regardless of their direction of emission. The existence of such a total spin transfer (A positive if photon and electron spin are parallel, negative for the antiparallel case) is also called the Fano effect. Though A is an averaged

† The angular dependence of $P(\theta)$ in the form of equation (2) has been experimentally verified by Schönhense (1980).

polarisation value, it is sometimes very high, up to 100% (Heinzmann *et al* 1970a, b) and sometimes shows a pronounced resonance structure as a function of the photon energy (Heinzmann *et al* 1975, 1976).

(v) Analogous to the differential cross section $Q(\theta)$, in the fifth type of experiment one looks at the angular dependence of the spin polarisation of photoelectrons in the direction of the fully or partially transferred photon spin

$$A(\theta) = \frac{A - \alpha(\frac{3}{2}\cos^2\theta - \frac{1}{2})}{4\pi Q(\theta)/Q}. \tag{3}$$

The parameter α describes the deviation of the differential spin polarisation $A(\theta)$ from an isotropic value A.

The experiments described in this paper are of types (iii) and (iv), i.e. measurements of ξ using unpolarised light and of A using circularly polarised light.

Some of these five measurements may be replaced by other experiments to obtain the same information about the photoionisation process; for example, in procedures (i), (ii) and (iii) the same parameters Q, β and ξ (but no more) are obtained if linearly polarised light instead of unpolarised is used in the experiments (Cherepkov 1974, 1979, Lee 1974). Or, instead of the measurement of the spin polarisation A in (iv), the same result can be obtained by measuring the asymmetry of Q for photoionisation of spin polarised *atoms* using left- and right-handed circularly polarised radiation (Baum *et al* 1972).

Nevertheless, there are some simple cases where it is not even necessary to perform five experiments. For example, a bound electron with $j = \frac{1}{2}$ is not able to make a transition into the continuum according to the selection rule $\Delta j = -1$. Therefore, such a photoionisation process (for example, for rare gases when the remaining ion is in the $^2P_{1/2}$ state) is determined by only two real matrix elements and one phase difference.

It may be worth noting here that the spin–orbit interaction is responsible for the existence of any spin polarisation of photoelectrons, whether this is produced by unpolarised radiation (P) or by a spin transfer from photon to electron (A). This will be discussed in more detail in II.

3. Measurement of the photoelectron polarisation for photoionisation of xenon atoms by unpolarised radiation

In order to observe the polarisation $P(\theta)$ one must detect photoelectrons emitted in a well defined direction θ, as pointed out in §2. Spin polarisation of photoelectrons ejected by unpolarised light from unpolarised targets was first found with lead atoms (Heinzmann *et al* 1978). But whereas in the lead experiment the photoelectron emission was resolved only for angle and spin, in the present experiment on xenon the emission is also measured as a function of the photon energy and the kinetic energy of the photoelectrons. The complication of such polarisation measurements is that they combine the intensity problems of photoelectron spin analysis with the difficulties of photoelectron angular- and energy-distribution experiments. Preliminary results have already been published elsewhere (Heinzmann *et al* 1979b).

The first two ionisation thresholds of xenon are in the VUV range: 12·13 eV or 102·2 nm (ionic ground state $^2P_{3/2}$) and 13·44 eV or 92·2 nm (excited ionic state $^2P_{1/2}$); it was, therefore, necessary to build new windowless VUV radiation sources yielding adequate intensity (more than 10^{11} photons/s) for this experiment. Capillary discharge

tubes yielding intense rare-gas resonance lines have been utilised as light sources; the radiation produced by a low-pressure discharge (pressure a few mbar, current 200 mA) in an Al_2O_3 capillary has been focused by a glass light capillary onto the target. In a test measurement using a double ionisation chamber of the Samson type (Samson 1964), the intensities of seven He and Ne resonance lines were found to be greater than 10^{11} photons/s (He I 8×10^{12} photons/s, for example). The results of these absolute intensity measurements as well as a detailed description of the radiation source is given elsewhere (Heinzmann and Schönhense 1979, 1980). It is worth noting that the main reason for the high radiation intensities was the very high purity of the rare-gas discharges: the gas inlet system used only UHV components, the source was metal sealed and heatable, and the impurities in the gas flowing through the lamp were much smaller than 1 ppm.

A schematic diagram of the whole apparatus used is shown in figure 2. Two VUV light sources are used, each giving a beam about 1·5 mm in diameter which crosses the atomic beam streaming from the nozzle to a liquid helium cryo-pump (2300 l s^{-1} speed for xenon) and is absorbed by a light detector on the other side of the ionisation tube. It is crucial for the reliability of the spin polarisation measurements that there are no residual fields in the ionisation chamber which could deflect the photoelectrons and thus lead to a spurious angle of emission. In order to check whether residual fields had been sufficiently suppressed, a great number of asymmetry parameters β have been measured at different photon energies using a third resonance lamp placed at an angle of $\theta = 16°$ (not shown in figure 2). The agreement of the β values measured for several noble gases and molecules (Schönhense 1978) with those found by other authors (Dehmer *et al* 1975, Miller *et al* 1977, Niehaus and Ruf 1972) confirmed the reliability of the angle-resolved spin-polarisation measurements.

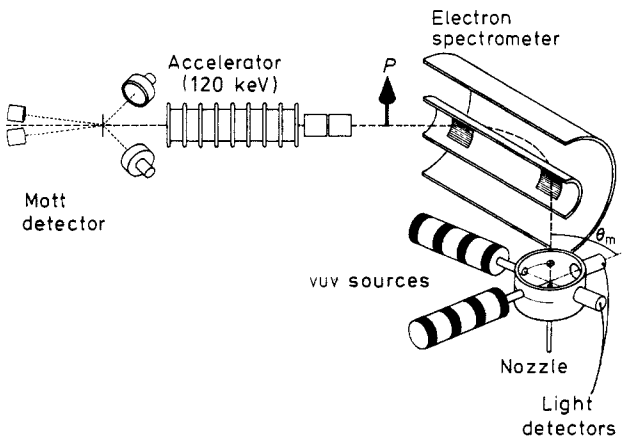

Figure 2. Schematic diagram of the apparatus for the measurement of ξ.

For these measurements the photoelectrons were observed at angles $\pm\theta_m$ with respect to the two light beams, where θ_m is the magic angle, 54° 44′, so-called because at this angle $Q(\theta) = Q/4\pi$ in equation (1) and the parameter ξ in equation (2) can be obtained without any knowledge of β. ξ is then found from $\xi = 1{\cdot}061\ P(\theta_m)$. Because according to equation (2) $P(-\theta_m) = -P(\theta_m)$ the sign of the spin polarisation could be changed once a minute by switching from one light source to the other.

The photoelectrons produced entered an electron spectrometer (cylindrical mirror analyser, radii 90 and 35 mm, widths of slits 1·5 mm, distance between slits 246 mm, angular acceptance ±5·5°, see Brandt 1975) with an energy resolution of 0·7% (but not smaller than 35 meV) full width at half maximum. One can therefore take into account the fact that beyond the second ionisation threshold (92·2 nm) photoelectrons of two distinct energies are produced for a single incident wavelength. These correspond, as pointed out above, to the two states $^2P_{3/2}$ and $^2P_{1/2}$ of the xenon ion, differing in energy by 1·3 eV. The use of an electron spectrometer is also essential because the resonance radiation coming from the source is always a mixture of light of different wavelengths. No radiation monochromator could be used because of intensity problems and therefore the electron spectrometer also had the function of analysing the photon-energy dependence of the photoelectron emission.

The photoelectrons selected by the spectrometer are focused on to the entrance of a 120 keV acceleration tube and finally hit the thin gold foil of a Mott detector for polarisation analysis. The spin polarisation is determined from the left–right asymmetry of the electron intensity scattered into the two counters at 120°. Instrumental asymmetries could easily be eliminated by taking advantage of the reversal of the spin polarisation once every minute. The two additional counters at small scattering angles allow further corrections for instrumental asymmetries to be made. A detailed description of the Mott detector used and of the procedure to measure the polarisation is given elsewhere (Heinzmann 1978).

Figures 3 and 4 show the polarisations measured for various wavelengths and the values of ξ resulting from these data. The polarisations of photoelectrons associated with the $^2P_{1/2}$ (figure 3) and $^2P_{3/2}$ (figure 4) states of the residual ion differ in sign. This shows the necessity of resolving the fine structure using the electron spectrometer since, otherwise, the polarisations would almost cancel one another. The polarisations P and thus the parameters ξ are different from zero and show a pronounced wavelength dependence. At a wavelength of about 50 nm they show a change in sign. The error bars drawn in figures 3 and 4 are the RMS sum of the single statistical error of the polarisation measurements and the uncertainty of the analysing power of the Mott detector (Sherman function = −0·26 ± 0·01). They include also a very small correction

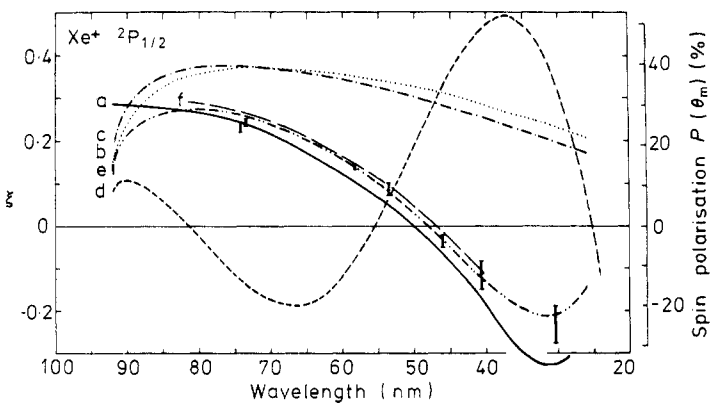

Figure 3. Experimental results (error bars) of polarisation (scale on the right) and for parameter ξ (scale on the left) for photoelectrons corresponding to the ionic state $^2P_{1/2}$. The curves follow from calculations using random phase approximation (curves a and f) and multichannel quantum defect theory (curves b–e).

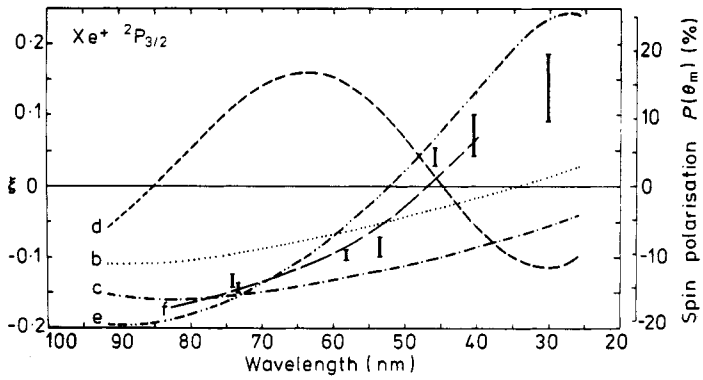

Figure 4. The same as figure 3 but for photoelectrons corresponding to the ionic state $^2P_{3/2}$.

for the angular divergence of ±5·5° of the photoelectrons accepted by the electron spectrometer.

Figures 3 and 4 also show a few theoretical results. Curve a (full curve) calculated by Cherepkov for the case $^2P_{1/2}$ using the random phase approximation with exchange was the first theoretical prediction in this wavelength range. It is worth noting that the curve of Cherepkov in figure 3 does not agree in sign with his published data (Cherepkov 1978) because there was an error in sign (N A Cherepkov, private communication). Curves f in figures 3 and 4 are the results of the latest calculation by Huang *et al* (1979) using a relativistic random phase approximation. The other curves have been calculated by means of the 'multichannel quantum defect theory', with use of various sets of parameters from the discrete spectral range, which I found in the literature. For curves b and c I used the data of Lee (Dill 1973) and Geiger (1976), respectively, with energy-independent eigen-quantum defects, matrix elements and transformation matrix (see II). Curves d are based upon the values of Geiger (1977) where the eigen-quantum defects and the matrix elements have been selected to be energy dependent in such a way as to fit the behaviour of *all* spectral lines in the discrete spectrum best. Curves e, which of all the theoretical curves drawn in figures 3 and 4 show the best agreement with the experimental results, were calculated from Geiger's data that gave the best fit for bound transitions into the *higher* Rydberg states only (J Geiger 1979, private communication). A detailed comparison of the data of the discrete and the continuous spectral range is given in II, where the matrix elements and the phase differences (quantum defects) are compared directly.

4. Measurement of the spin polarisation of photoelectrons produced from xenon atoms by circularly polarised synchrotron radiation

4.1. Apparatus

Experimental studies of the polarisation A of photoelectrons produced by circularly polarised radiation (see experiment (iv) in § 2) are hampered by the fact that most atoms have their ionisation thresholds in the VUV, where conventional methods for producing circularly polarised radiation of high intensity breakdown. Such experiments with circularly polarised light (Heinzmann *et al* 1979a) can, however, be performed with synchrotron radiation. Normally this is linearly polarised if emitted in

the plane of the synchrotron (Haensel and Kunz 1967, Codling 1973), but nearly 30 years ago Olsen (1952) and Westfold (1959) showed theoretically that the radiation emitted above and below the synchrotron plane contains a large fraction of circular polarisation. This is due to the fact that the two linearly polarised components (oscillating in and perpendicular to the synchrotron plane) should be coherently superimposed with a phase difference of 90°, but the component perpendicular to the plane is emitted only into directions above and below the plane. The present work is the first time that circular polarisation of synchrotron radiation has been measured in the VUV and used experimentally.

Because the theory describing synchrotron radiation is based upon only one electron circulating in a synchrotron or storage ring, there have been some doubts about its validity in practice. In reality the current in the synchrotron is many mA and the electron beam has a diameter of one or more mm and produces betatron oscillations in the vertical direction.

The experiment described in this section was performed with the 2·5 GeV synchrotron at Bonn, because the vertical angular range in which the circularly polarised radiation is emitted is smaller than with smaller machines. On the other hand, it was possible to position the apparatus very near to the tangent point of the synchrotron. A schematic diagram of the apparatus is shown in figure 5. A 10 m normal-incidence monochromator with a concave mirror (diameter 250 mm, radius 10 m) which produces a one to one image of the electron beam in the exit slit was built. This monochromator does not possess an entrance slit because of its high horizontal angular acceptance (22 mrad). At a distance of 6·13 m to the tangent point there is a rotatable plane grating (150 × 50 mm) in a Littrow mounting. This mounting and the normal-incidence reflection at the mirror have been selected in order to avoid

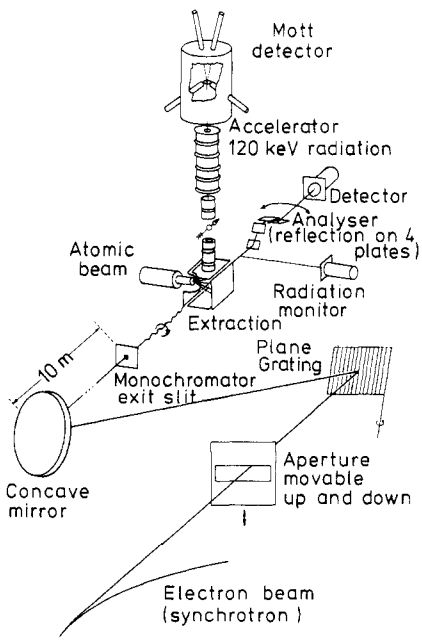

Figure 5. Schematic diagram of the apparatus for the measurement of A.

depolarisation effects which would be induced by non-normal-incidence reflections on the optical components.

Before finalising the design of the grating, Dr Neviere (Laboratoire d'Optique Electromagnetique, University Marseille) calculated the effect of the grating on the polarisation of the radiation to be monochromatised (Loewen and Neviere 1978, Loewen *et al* 1977, M Neviere, private communication). This was especially important at wavelengths where so-called 'Wood anomalies' arise (Mount and Fastie 1978, Polushkin *et al* 1976, Cowan and Arakawa 1977, Hutley 1973, McPhedran and Watersworth 1973). In order to keep the depolarisation effects as small as possible a holographic grating (4960 sinusoidal rules per mm, ruling depth equal to 0·1 times the ruling separation, platinum overcoated) was chosen.

The monochromator covers the wavelength range between 40 and 180 nm (highest efficiency at about 70 nm) and has a linear dispersion in the plane of the exit slit of 30·4 $[1-(\lambda/403\ \text{nm})^2]^{-1/2}$ mm/nm. Thus, in the wavelength range described above the bandwidth of the radiation coming from the electron beam in the synchrotron (about 1·5 mm broad) through the 1·5 mm opened exit slit is 0·05 nm. This has been experimentally verified by use of a second VUV monochromator for calibration. The plane grating can be rotated by steps of 2×10^{-3} degrees resulting in steps of 0·013 nm wavelength.

The radiation coming from the electron beam is cut off in the vertical direction by an aperture which can be moved up and down for selecting radiation of left or right circular polarisation. In order to protect the grating against radiation damage this aperture normally excluded vertical angular ranges within ±1 mrad, because the harder x-ray components are emitted in a narrower vertical range than the VUV radiation of interest. For the same reason, for these experiments the 2·5 GeV synchrotron was always run at only 0·8 GeV. Finally, it is worth noting that the vacuum in the region of the grating was better than 10^{-8} mbar.

In the wavelength range described the intensity of the circularly polarised radiation behind the exit slit was measured, using a double ionisation chamber of the Samson type (Samson 1964), to be between 10^9 and 10^{10} photons/s. A detailed description of this absolute intensity measurement as well as of some optical polarisation measurements will be given elsewhere (Heinzmann *et al* 1981). The intensities of all the higher orders coming through the monochromator exit slit were eight times weaker than that of the first order. This was measured by observing the photoelectron intensities emitted by xenon atoms above and below the photoionisation threshold and taking into account the decrease of the photoionisation cross section with decreasing wavelength.

The polarisation of the radiation passing through the atomic beam was measured by a rotatable linear analyser by means of successive reflections from four gold mirrors at angles of 60° as shown in figure 5. According to the calculations of Hunter (1978), based upon the experimentally well known optical constants, the analysing power of this arrangement should be better than 98·8% in the wavelength range between 40 and 180 nm. The intensity was measured with an open photomultiplier, and a second such multiplier was used as a monitor to make the measurement of the circular polarisation independent of fluctuations of the radiation intensity.

Because the analyser cannot distinguish between circular and unpolarised radiation, the percentage of unpolarised background radiation was measured: in this measurement an additional MgF_2 quarterwave plate, described by Heinzmann (1977), was used to transform the elliptical polarisation into a linear one which was analysed by the four-mirror arrangement. The maximum linear polarisation was found at a wavelength

8 nm away from the nominal wavelength (150 nm) for which the quarterwave plate was designed, indicating that the phase difference between the components of the synchrotron radiation coming through the exit slit is 86° rather than 90°. The effect on the circular polarisation of this phase shift is negligible since it corresponds to a depolarisation factor of only 0·998. From the maximum value of the linear polarisation, it was established that the fraction of unpolarised background was smaller than 1% and the analysing power was at least 99%.

The measured percentage circular polarisation of the radiation emitted into the two vertical angular ranges from 1 to 3·5 mrad and 0 to 3·5 mrad respectively is shown in figure 6 as a function of wavelength. The circular polarisation is nearly wavelength independent; it is about 10% smaller than the values calculated using the 'pure' theory of synchrotron radiation neglecting betatron oscillations and the finite size of the electron beam.

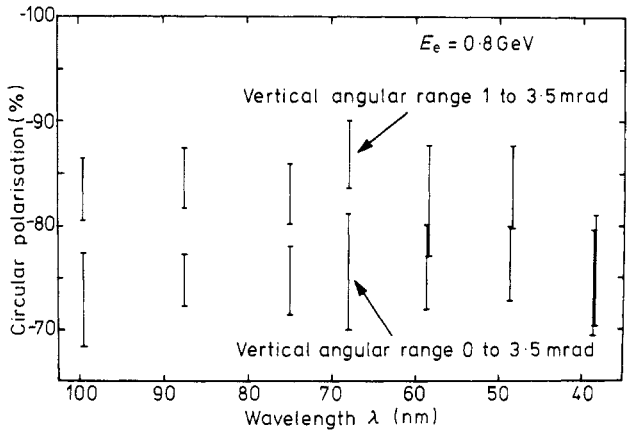

Figure 6. Measured circular polarisation of radiation emitted into angular ranges from 1 to 3·5 mrad and 0 to 3·5 mrad with respect to the synchrotron plane.

The atomic beam was produced by a focusing capillary array (10^7 capillaries, 5 μm diameter and 2·5 mm long, focus 50 mm) described by Lucas (1973a, b). The photoelectrons produced in the target ($6 \times 6 \times 6$ mm^3, about 10^{12} atoms) were extracted by an electrostatic quadrupole lens (Heinzmann 1978) independently of their direction of emission, focused by electron optical components and accelerated to 120 keV for polarisation analysis in a Mott detector (Heinzmann 1978). Spin polarisation and optical polarisation measurements could be performed simultaneously. All spin polarisation results shown in the figures are the ratios of the measured spin polarisations to the measured optical polarisations.

4.2. Experimental results and comparison with theory

The results measured in the autoionisation range between 102·2 and 92·2 nm are shown in figure 7. The full curve in the upper part of figure 7 represents the photoelectron intensities obtained. The shape of the curve as well as the positions of the resonance maxima and minima observed are in good agreement with the well known photoionisation cross section measured by Saile (1976) and Huffmann *et al* (1963). This

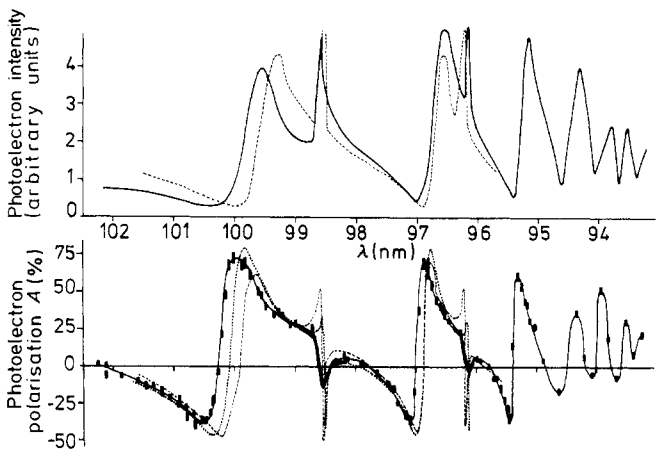

Figure 7. Photoionisation in the autoionisation region. Upper part, photoelectron intensity; lower part; spin polarisation A; full curves, experimental results; broken curves, theoretical predictions by Lee (1974); dotted curve, theoretical results according to Geiger's data (see text).

indicates that the bandwidth of 0·05 nm used was adequate for observation of even the narrow resonances. Furthermore, it shows that the steps of 2×10^{-3} degrees in grating rotation do indeed correspond to steps of 0·013 nm in wavelength.

In the lower part of figure 7 the measured polarisation data are shown as black rectangles. They are connected by the full curve in order to indicate that the polarisation also shows a pronounced resonance structure (changing from −40% to +75% in a wavelength range smaller than 1 nm). The base of each rectangle is the bandwidth of the radiation used, and the height represents the error bar for the polarisation including the uncertainties of light polarisation measurement, spin polarisation analysis (single statistical error) and analysing power of the Mott detector (Sherman function).

The broken curves in the upper and the lower part of figure 7 are the predictions of Lee (1974). Although the shapes of the theoretically predicted and the measured curves are very similar, there are some discrepancies between Lee's prediction and the measured values in the positions of the broad resonances, e.g. at 100 nm. These can be seen not only in the cross section and the spin polarisation but also in the asymmetry parameter β of the angular distribution measured by Samson and Gardner (1973).

The dotted line in the lower part of figure 7 has been calculated by means of the 'multichannel quantum defect theory', using the same set of parameters from the discrete spectral range (J Geiger 1979, private communication) that yielded the best agreement with the experimental results in the calculation of ξ (curves e in figures 3 and 4). These calculated results agree better with the measured data than do those of Lee. Nevertheless, there remains a small discrepancy between theory and experiment near 100 nm, which cannot be explained at the moment.

The shape of the narrow polarisation resonance at 98·6 nm is shown in figure 8 using an expanded wavelength scale. Typical error bars are indicated at three points only. Again, the dotted line obtained by means of the 'multichannel quantum defect theory' using Geiger's data shows a discrepancy between theory and experiment in the position of the resonance. However, this shift is 2·5 times smaller than the corresponding shift at the broader resonance at 100 nm. In order to show that this shift is not due to a wrongly

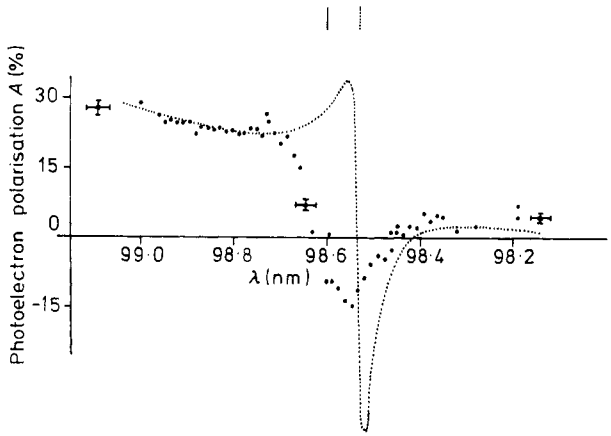

Figure 8. Spin polarisation A at the narrow resonance near 98·6 nm. Points and error bars are the measured polarisations. The dotted line represents the calculation by means of MQDT using Geiger's data. The vertical lines indicate the positions of the cross section resonance peak according to experiment (full) and theory (dotted).

calibrated wavelength scale in this experiment, the positions of the cross section resonance peaks are shown by vertical lines at the top of figure 8, full for the experimental value (Saile 1976) and dotted for the value calculated from Geiger's data. The discrepancy in the depth of the polarisation curve (negative values) between theory and experiment could possibly be explained by insufficient resolution of the polarisation peak in the experiment, but may also be a real effect.

Figure 9 shows the measured spin polarisation beyond the second threshold at a number of wavelengths between 92 and 45 nm, at some of which measurements of ξ have also been performed (figures 3 and 4). In this wavelength range, photoelectrons corresponding to the two† residual ionic states were obtained so that the results shown in figure 9 are mean values for both kinds of electrons, which have polarisation of opposite sign (Cherepkov 1974). Nevertheless, the polarisation of the two kinds of electrons can be determined separately directly from the experimental data, as shown in II.

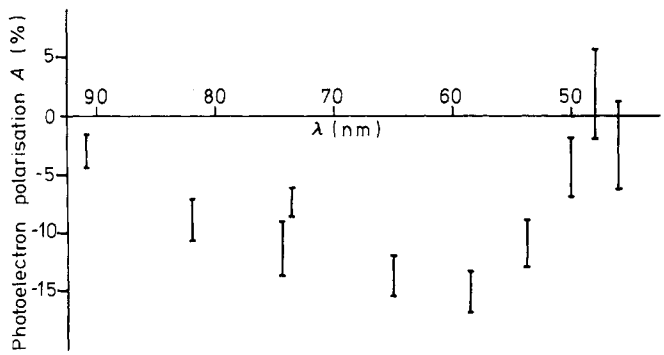

Figure 9. Measured spin polarisation A beyond the second threshold.

† At wavelengths shorter than 53 nm there are also photoelectrons resulting from a 5s transition (third ionisation threshold). Their influence, however, is negligible because of the 40 times smaller photoionisation cross section (Samson and Gardner 1974).

Acknowledgments

The author wishes to express his gratitude to Professor Dr J Kessler, Professor Dr G Nöldeke and Professor Dr W Paul who strongly supported the projects from the very beginning. Especially I should like to thank my coworkers F Schäfers, G Schönhense, Dr K Thimm and A Wolcke for their intensive encouragements in performing the experiments. Furthermore, I thank Dr D Husmann and Dr J Hormes for their interest and help and Dr M Neviere for the calculation of the grating data. The author is also grateful to all colleagues of the workshops in Bonn and Münster for their technical assistance in building the apparatus. I thank Dr D Burgess and Dr A Thorne for reading the manuscript and the great hospitality during my stay at the Imperial College London. Support by the University of Bonn, the University of Münster, the Deutsche Forschungsgemeinschaft and the Bundesminister für Forschung und Technologie is gratefully acknowledged.

References

Baum G, Lubell M S and Raith W 1972 *Phys. Rev.* A **5** 1073–87
Brandt D 1975 *Diplomarbeit* Universität Münster
Cherepkov N A 1974 *Sov. Phys.-JETP* **38** 463–9
—— 1978 *J. Phys. B: Atom. Molec. Phys.* **11** L435–9
—— 1979 *J. Phys. B: Atom. Molec. Phys.* **12** 1279–96
Codling K 1973 *Rep. Prog. Phys.* **36** 541–624
Cowan J J and Arakawa ET 1977 *Opt. Commun.* **21** 428–31
Dehmer J L, Chupka W A, Berkowitz J and Jivery W T 1975 *Phys. Rev.* A **12** 1966–73
Dill D 1973 *Phys. Rev.* A **7** 1976–87
Fano U 1969a *Phys. Rev.* **178** 131–6
—— 1969b *Phys. Rev.* **184** 250–1
Geiger J 1976 *Z. Phys.* A **276** 219–24
—— 1977 *Z. Phys* A **282** 129–41
Haensel R and Kunz C 1967 *Z. Angew. Phys.* **23** 276–95
Heinzmann U 1977 *J. Phys. E: Sci. Instrum.* **10**, 1001–5
—— 1978 *J. Phys. B: Atom. Molec. Phys.* **11** 399–412
—— 1980 *J. Phys. B: Atom. Molec. Phys.* **13** 4367–85
Heinzmann U, Heuer H and Kessler J 1975 *Phys. Rev. Lett.* **34** 441–4
—— 1976 *Phys. Rev. Lett.* **36** 1444–7
Heinzmann U, Kessler J and Lorenz J 1970a *Phys. Rev. Lett.* **25** 1325
—— 1970b *Z. Phys.* **240** 42–61
Heinzmann U, Osterheld B and Schäfers F 1981 to be published
Heinzmann U, Schäfers F, Thimm K, Wolcke A and Kessler J 1979a *J. Phys. B: Atom. Molec. Phys.* **12** L679–83
Heinzmann U and Schönhense G 1979 *Proc. 11th Int. Conf. on Physics of Electronic and Atomic Collision* (Kyoto: Society for Atomic Collision Research) Abstracts p 24–5
—— 1980 to be published
Heinzmann U, Schönhense G and Kessler J 1979b *Phys. Rev. Lett.* **42** 1603–5
Heinzmann U, Schönhense G and Wolcke A 1978 *Proc. Int. Workshop on Coherence and Correlation in Atomic Collisions, London* ed H Kleinpoppen and J Williams (New York: Plenum) Abstracts p 607–12
Huang K-N, Johnson W R and Cheng K T 1979 *Phys. Rev. Lett.* **43** 1658–61
Huffmann R E, Tanaka Y and Larrabee J C 1963 *J. Chem. Phys.* **39** 902–9
Hunter W R 1978 *Appl. Opt.* **17** 1259–70
Hutley M C 1973 *Opt. Acta* **20** 607–24
Kessler J 1976 *Polarized Electrons* (Berlin: Springer) p 123–46
Lee C M 1974 *Phys. Rev.* A **10** 1598–604
Loewen E G and Neviere M 1978 *Appl. Opt.* **17** 1087–92

Loewen E G, Neviere M and Maystre D 1977 *Appl. Opt.* **16** 2711–21
Lucas C B 1973a *J. Phys. E: Sci. Instrum.* **6** 991–4
—— 1973b *Vacuum* **23** 395–402
McPhedran R C and Watersworth M D 1973 *Opt. Acta* **20** 533–47
Miller D L, Dow J D, Houlgate R G, Marr G V and West J B 1977 *J. Phys. B: Atom. Molec. Phys.* **10** 3205–13
Mount G H and Fastie W G 1978 *Appl. Opt.* **17** 3108–16
Niehaus A and Ruf M W 1972 *Z. Phys.* **252** 84–94
Olsen H 1952 *Kgl. Norske Vidensk. Selsk. Skrifter* No 5
Polushkin Yu, Stanevich A E and Fomina T N 1976 *Sov. J. Opt. Technol.* **43** 81–4
Saile V 1976 *Dissertation* Universität München
Samson J A R 1964 *J. Opt. Soc. Am.* **54** 6
Samson J A R and Gardner J L 1973 *Phys. Rev. Lett.* **31** 1327–30
—— 1974 *Phys. Rev. Lett.* **33** 671–3
Schönhense G 1978 *Diplomarbeit* Universität Münster
—— 1980 *Phys. Rev. Lett.* **44** 640–3
Westfold K C 1959 *Astrophys. J.* **130** 231